doi:10.1111/j.1558-5646.2012.01626.x

LATE PALEOZOIC FUSULINOIDEAN GIGANTISM DRIVEN BY ATMOSPHERIC HYPEROXIA

Jonathan L. Payne,[1,2] John R. Groves,[3] Adam B. Jost,[1] Thienan Nguyen,[4] Sarah E. Moffitt, Tessa M. Hill,[6] and Jan M. Skotheim[4]

[1]*Department of Geological and Environmental Sciences, Stanford University, 450 Serra Mall, Building 320, Stanford, California 94305*

[2]*E-mail: jlpayne@stanford.edu*

[3]*Department of Earth Science, University of Northern Iowa, Cedar Falls, Iowa 50614-0335*

[4]*Department of Biology, Stanford University, Stanford, California 94305*

[5]*Bodega Marine Laboratory and Graduate Group in Ecology, University of California Davis, Bodega Bay, California 94923*

[6]*Department of Geology and Bodega Marine Laboratory, University of California Davis, Davis, California 95616*

Received October 19, 2011
Accepted February 28, 2012
Data Archived: Dryad: doi:10.5061/dryad.d37p59vg

Atmospheric hyperoxia, with pO_2 in excess of 30%, has long been hypothesized to account for late Paleozoic (360–250 million years ago) gigantism in numerous higher taxa. However, this hypothesis has not been evaluated statistically because comprehensive size data have not been compiled previously at sufficient temporal resolution to permit quantitative analysis. In this study, we test the hyperoxia-gigantism hypothesis by examining the fossil record of fusulinoidean foraminifers, a dramatic example of protistan gigantism with some individuals exceeding 10 cm in length and exceeding their relatives by six orders of magnitude in biovolume. We assembled and examined comprehensive regional and global, species-level datasets containing 270 and 1823 species, respectively. A statistical model of size evolution forced by atmospheric pO_2 is conclusively favored over alternative models based on random walks or a constant tendency toward size increase. Moreover, the ratios of volume to surface area in the largest fusulinoideans are consistent in magnitude and trend with a mathematical model based on oxygen transport limitation. We further validate the hyperoxia-gigantism model through an examination of modern foraminiferal species living along a measured gradient in oxygen concentration. These findings provide the first quantitative confirmation of a direct connection between Paleozoic gigantism and atmospheric hyperoxia.

KEY WORDS: **Body size, Carboniferous, Cope's Rule, foraminifera, oxygen, Permian.**

The general phenomenon of evolution toward large size has attracted considerable interest since Cope (1871) noted phylogenetic trends toward increased body size in many animal groups. Gigantism was particularly widespread during the late Paleozoic (360–250 million years ago, Mya), including many of the largest fossil insects, brachiopods, and foraminifera (Newell 1949; Graham et al. 1995). Although Newell (1949) and many other workers (e.g., Simpson 1944; Alroy 1998; Kingsolver and Pfennig 2004; Clauset and Erwin 2008) have advocated ecological selective pressures favoring larger individuals as the primary drivers of gigantism, the prevalence of unusually large organisms during the Carboniferous and Permian periods has prompted speculation that high atmospheric oxygen concentrations played a critical role in enabling gigantism (Rutten 1966; Graham et al. 1995; Dudley 1998; Berner et al. 2007). In fact, prior to the development of geochemical model reconstructions of atmospheric composition (e.g., Schidlowski et al. 1977; Schidlowski and Junge 1981; Berner 1987; Berner and Canfield 1989; Berner 2006), gigantism

EVOLUTION
INTERNATIONAL JOURNAL OF ORGANIC EVOLUTION

was viewed by some as the best geological evidence for Permo–Carboniferous hyperoxia (Rutten 1966).

Despite abundant circumstantial evidence, however, a direct link between Permo–Carboniferous gigantism and atmospheric hyperoxia has yet to be demonstrated through either statistical correlation or physiological modeling. The alternative possibilities that size increase reflects either an ecologically driven trend or simple random drift away from the small sizes of the last common ancestors of the clades in question (Stanley 1973; Gould 1988; McShea 1994) have not been ruled out. In fact, quantitative assessment of oxygen transport in dragonflies shows the decrease in maximum size from the Permian to the Recent is far too large to be explained simply by a decline in atmospheric pO_2, suggesting size decrease may have been driven more by the advent of flying vertebrate predators than by environmental change (Okajima 2008). The structural complexity of the arthropod tracheal system and its limited preservation in Carboniferous and Permian dragonflies prevent detailed prediction of overall maximum size from physiological modeling alone, leaving unanswered the question of whether the largest Permian dragonflies had in fact reached oxygen-imposed upper bounds on size. Consequently, the relative importance of environmental change versus ecological interactions in driving the evolution of unusually large organisms during the late Paleozoic remains poorly understood.

In this study, we consider the case of gigantism within fusulinoidean foraminifers (Order Fusulinida; Superfamily Fusulinoidea). Fusulinoideans are perhaps the best-recognized case of evolution toward large size in marine protists (Newell 1949; Dunbar 1963; Douglass 1977) and they are among the largest single-celled organisms preserved in the fossil record (Newell 1949; Payne et al. 2009). Their fossil record has been studied extensively and catalogued due to their importance in biostratigraphy and petroleum geology. Fusulinoideans originated late in the Mississippian (~325 Mya) and became spectacularly large, diverse, and abundant prior to their demise during the end-Permian mass extinction (~252 Mya). Because large variations in atmospheric oxygen concentration (pO_2) occurred during fusulinoidean evolution (Berner 2006), and because fusulinoideans lack the complex respiratory and circulatory structures that complicate quantitative assessment of the link between pO_2 and size in animals through physiological modeling, they are an ideal test case for examining the influence of atmospheric pO_2 on size evolution.

Scaling Analysis

Fusulinoidean foraminifera are among the largest protists in the fossil record; the largest individuals achieved lengths of more than 10 cm and thicknesses on the order of 10 mm (Stevens 1995). Experiments show that the fitnesses of animal egg masses of similar dimension are commonly influenced by oxygen availability (Strathmann and Strathmann 1995; Fernandes and Podolsky 2011). A scaling analysis confirms that oxygen availability may impose physiological constraints on foraminiferan size and shape within the range of observed values. Oxygen may be transported within foraminifers via diffusion or active transport (cytoplasmic streaming). To determine which of these mechanisms is dominant, we consider their relative time scales in a foraminifer of smallest dimension $L \sim 1$ mm. The time, τ_d, for O_2 to diffuse through the cell will be $\tau_d \sim L^2/D$, $\sim 10^4$ sec, where $D \sim 10^{-4}$ mm^2/sec is the diffusion constant for O_2 in cytoplasm (White 1974). Large foraminifers have been reported to exhibit cytoplasmic streaming with velocity $u \sim 5 \cdot 10^{-3}$ mm/sec (Travis and Bowser 1991) so that the time to transport O_2 across the cell is $\tau_t \sim L/u \sim 10^2$ sec $<<$ τ_d, indicating that cytoplasmic streaming is the dominant oxygen transport mechanism in millimeter-sized foraminifers. Because τ_d scales with L^2 whereas τ_t scales with L, the dominance of mixing over diffusion was likely higher in the largest fusulinoideans. Of course, oxygen must still diffuse across the cell membrane to enter the cell and across the mitochondrial membranes to be used in respiration. These steps are critical from the standpoint of cell physiology, but the permeability of these membranes to oxygen is similar to that of water (Subczynski et al. 1989) and in vivo measurements show that oxygen concentrations do not differ significantly across cell and mitochondrial membranes (Subczynski et al. 1991). Consequently, these membranes do not present significant barriers to oxygen transport (Subczynski and Swartz 2005) and their effects can be safely ignored for the purposes of our scaling analysis.

Assuming active transport, we may estimate the largest permitted volume (V) to surface area (SA) ratio for a foraminifer as a function of O_2 consumption rate per unit mass given fixed specific metabolic rate and cytoplasmic streaming velocity. We emphasize that this calculation is not intended to predict a maximum possible size for foraminifera as a function of oxygen availability; larger cells are always permitted if they exhibit lower metabolic rates or higher cytoplasmic streaming rates. Rather, this calculation predicts contours of approximately equivalent fitness produced by the interacting constraints of oxygen availability and metabolic rate. Observations of living foraminifers indicate specific metabolic rates, $r \sim 10^{-13}$ mol/sec·mm^3 (Geslin et al. 2011). Oxygen transport across the cell surface, $SA \cdot u \cdot [O_2]$ must exceed oxygen consumption, $V \cdot r$. Here, $[O_2] \sim 2 \times 10^{-10}$ mol/mm^3 is the oxygen concentration in seawater at 25°C (typical of shallow tropical marine habitats) at modern atmospheric pO_2 (21%). Given fixed rates of aerobic metabolism and cytoplasmic streaming, this relationship allows us to estimate the potential for extracellular oxygen concentrations to place physiological limitations on the V/SA ratio, $\max [V/SA] \sim L \sim u \cdot [O_2]/r \sim (10^{-3}$ mm/sec)

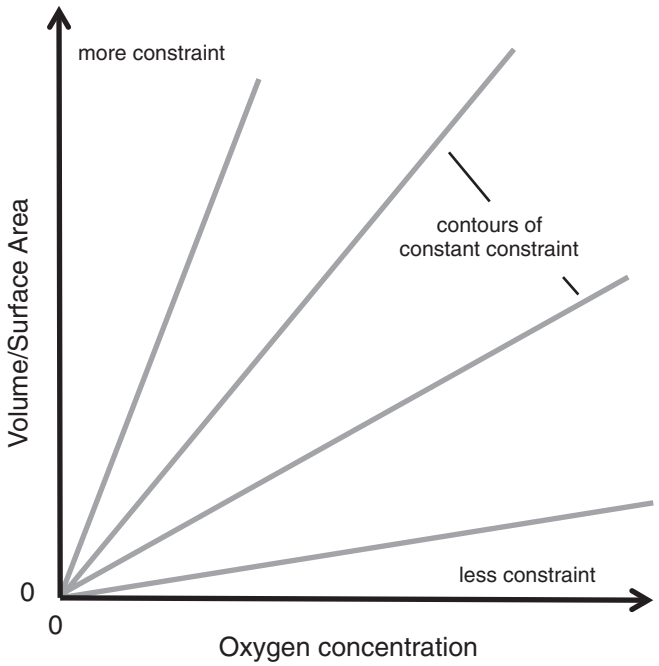

Figure 1. Conceptual illustration of physiological constraint imposed on volume to surface area ratio as a function of oxygen availability, assuming constant rates of cytoplasmic streaming and aerobic metabolism per unit volume. Contours of equivalent constraint on the ratio of volume to surface area increase linearly with oxygen availability. In other words, selective pressures imposed by oxygen demand are reduced as oxygen availability increases.

$(2\times10^{-10}$ mol/mm^3)/(10^{-13} mol/sec·mm^3) $\sim$ 2 mm. This scaling argument shows that physiological transport limits can affect the fitness of millimeter-sized foraminifers and that contours of equivalent fitness increase linearly with oxygen availability (Fig. 1), all else being equal. For example, a 1-mm thick cell at 15% pO_2 experiences a similar physiological oxygen constraint as a 2-mm thick cell at 30% pO_2. Accounting for allometric scaling of specific metabolic rate would alter the shape of these contours, but not the potential for oxgyen availability to influence fitness. Of course, the maximum size achieved by foraminifera at any given time and in any given place depends not only on oxygen availability but also on the other ecological and physiological pressures affecting cell size.

Material and Methods

To assess controls on size evolution in fusulinoidean foraminifera, we compiled four datasets of foraminiferan size: (1) a taxonomically standardized dataset of fossil fusulinoideans from North America compiled from the primary literature; (2) a global dataset of fossil fusulinoidean sizes measured from illustrations in the Ellis and Messina catalogue of foraminifera; (3) a regional dataset of extant foraminifera from the Sahul Shelf, between Australia and Timor, measured from illustrations in a published monograph; and (4) a local dataset of foraminiferan sizes measured from Quaternary core samples of the Santa Barbara Basin. We used the fossil datasets to evaluate evolutionary trends in fusulinoidean sizes. We used the modern datasets to further assess the influence of oxygen availability on foraminferan size and shape. All data reported herein are archived at Dryad (doi:10.5061/dryad.d37p59vg).

NORTH AMERICAN FUSULINOIDEAN DATA

Evolutionary trends in volume and volume/surface area in North American fusulinoideans were evaluated by compiling dimensional data for associations of species chosen to represent each successive geochronologic age from the beginning of Pennsylvanian time through the end of the Middle Permian. The association for each time interval was selected from the composite standard database of Groves and Wang (2009). Associations for the Morrowan, Leonardian, Roadian, Wordian, and Capitanian ages include only 13, 34, 23, 18, and 20 species, respectively, corresponding to all of the validly named species for those times of unusually low fusulinoidean diversity. Associations for all other ages comprise more than 35 species. Associations for high-diversity ages were selectively chosen to contain not only the most commonly occurring species, but also those representing extremes of size and shape. For example, the selected association for the Virgilian Age consists of 41 species, whereas more than 150 named species are known to occur in Virgilian strata. All of the species not included in the Virgilian analysis are large forms in the genera *Triticites*, *Leptotriticites,* and *Schwagerina*. Adding these species to the analysis would not affect the maximum or minimum observed size, but it would increase the mean and median size. The dataset does not include Late Permian species because there are no fusulinoidean-bearing, Upper Permian rocks in cratonic North America. This dataset has the advantage that it is taxonomically standardized and that species' stratigraphic ranges are well known, allowing them to be included in multiple stages where appropriate. In total, the dataset contains 345 occurrences of 270 species across 11 stages.

GLOBAL FUSULINOIDEAN DATA

To further test whether patterns observed in the North American dataset were representative of global processes, we compiled a global database of fusulinoidean species sizes from the Ellis and Messina catalog of foraminiferan species (Ellis and Messina 1940), which includes illustrations and descriptions of type material. Geological ages were assigned based upon the geochronologic age to which the type material belongs. Age assignments followed the timescale of Ogg et al. (2008). Specimens for which the type material was not resolved to a geochronologic age were excluded from the analysis. The vast scope of this database

limits the feasibility of taxonomic standardization or the determination of stratigraphic ranges for species that exist in multiple geochronologic ages. Despite these weaknesses, the Ellis and Messina dataset has the advantage of providing global coverage and sizes for Late Permian species that are absent from North America. In total, the global dataset contains 1823 species across 10 geological stages.

SAHUL SHELF DATA

The Sahul Shelf database was compiled from Loeblich and Tappan's (1994) comprehensive monograph of foraminifers from core-top samples. All illustrated specimens were measured, and the water depth for each specimen was assigned based upon the sample from which it was recovered. Each species was illustrated by one to three specimens obtained from different samples. One specimen of *Fijiella simplex* reported from 314-m water depth was excluded from the analysis because this species typically inhabits reef flat environments (Coulbourn and Resig 1975) and was therefore almost certainly transported substantially downslope prior to collection. Seawater oxygen concentration data were obtained from locality 35 in Fieux et al. (1994), which is the nearest measured site to the study area. Oxygen concentration along the Sahul Shelf decreases from atmospheric equilibrium in shallow waters to approximately half that value at 500-m depth (Fieux et al. 1994). Because the relationship between water depth and oxygen availablity is relatively consistent across the Sahul Shelf region (cf. Fig. 10b in Fieux et al. 1994), it is unlikely that this approximation is a substantial source of error in our analysis. In total, the Sahul Shelf dataset contains 1843 illustrated specimens representing 883 species and subspecies living at water depths less than 500 m.

SANTA BARBARA BASIN DATA

Santa Barbara Basin samples were collected aboard the R/V *Marion Dufresne* in 2002 and R/V *Melville* in 2008 using jumbo piston cores. Foraminifera were selected from the early deglaciation section of core MV0811-15JC (418 m water depth; 920–921 cm core depth; 16.4 ka) and the early Holocene section of core MD02-2503 (570 m water depth; 176–178 cm core depth; 7.2 ka). Sample ages based on linear interpolation between radiocarbon ages and tie points to other cores. Core sections were disaggregated and washed with deionized water prior to analysis. Modern seawater-dissolved oxygen concentrations at these depths in the modern Santa Barbara Basin fall below 1/10th of tropical sea-surface values. These values were used (Sholkovitz and Gieskes 1971) in our anlaysis because paleoceanographic evidence suggests Holocene values should be broadly similar to the modern (Ivanochko and Pedersen 2004). Oxygen concentrations may have been somewhat higher during early deglaciation, but the composition of the foraminiferan community indicates that it would not have approached fully oxygenated conditions. In total, the Santa Barbara Basin dataset contains 408 specimens representing 12 genera.

CALCULATION oF VOLUME aND SURFACE AREA

Test volume and surface area were calculated assuming a three-dimensional ellipsoid. Volume was therefore calculated as $4/3 \cdot \pi \cdot a \cdot b \cdot c$ where a, b, and c represent the radii. The surface area of a generalized three-dimensional ellipsoid cannot be determined using any simple analytical formula (Poelaert et al. 2011) and was therefore calculated using the approximation: $4 \cdot \pi \cdot [(a^z \cdot b^z + a^z \cdot c^z + b^z \cdot c^z)/3]^{1/z}$ where $z = 1.6075$, for which the maximum relative error is only slightly more than 1% (http://www.numericana.com/answer/ellipsoid.htm#thomsen). This error amounts to 0.004 $\log_{10}$ units, and is undoubtedly smaller than measurement error or the error associated with the ellipsoidal approximation of test shape. Thus, alternative approximations with exact formulae, such as prolate or oblate spheroids, would yield indistinguishable results.

ATMOSPHERIC pO_2 DATA

Atmospheric pO_2 at the midpoint of each geochronologic age was obtained from Berner's (2006) GEOCARBSULF model and rounded to the nearest percent. GEOCARBSULF uses geochemical records of carbon and sulfur isotopes to calculate fluxes in the global carbon and sulfur cycles over the past 600 million years and thereby constrain temporal variation in atmospheric oxygen and carbon dioxide levels. This calculation is possible because the carbon and sulfur cycles are the major controls on earth's surface redox state over geological time. We chose this model because the model results are broadly consistent with a range of independent geochemical proxy data for pCO_2 (Royer et al. 2004), as well as with independent calculations of atmospheric oxygen levels determined by estimating carbon cycle fluxes through direct determination of rock volumes rather than proxy measurements of carbon isotopes (Berner and Canfield 1989). In Berner (2006), the GEOCARBSULF results are reported relative to absolute age (in millions of years), rather than to stage boundaries. We used the stage midpoints based on the Gradstein and Ogg (1996) time scale employed by Berner (2006) to estimate pO_2 for each stage, but report these values relative to the Ogg et al. (2008) time scale in our figures because substantial improvements have occurred in the absolute age model for Carboniferous and Permian stages since the publication of the Gradstein and Ogg (1996) time scale.

STATISTICAL ANALYSIS

We used methods developed by Hunt (2006; Hunt et al. 2010) to determine the mode of size evolution in fusulinoideans, evaluating statistical support across four evolutionary models: (1) random walk; (2) directional evolution; (3) stasis;

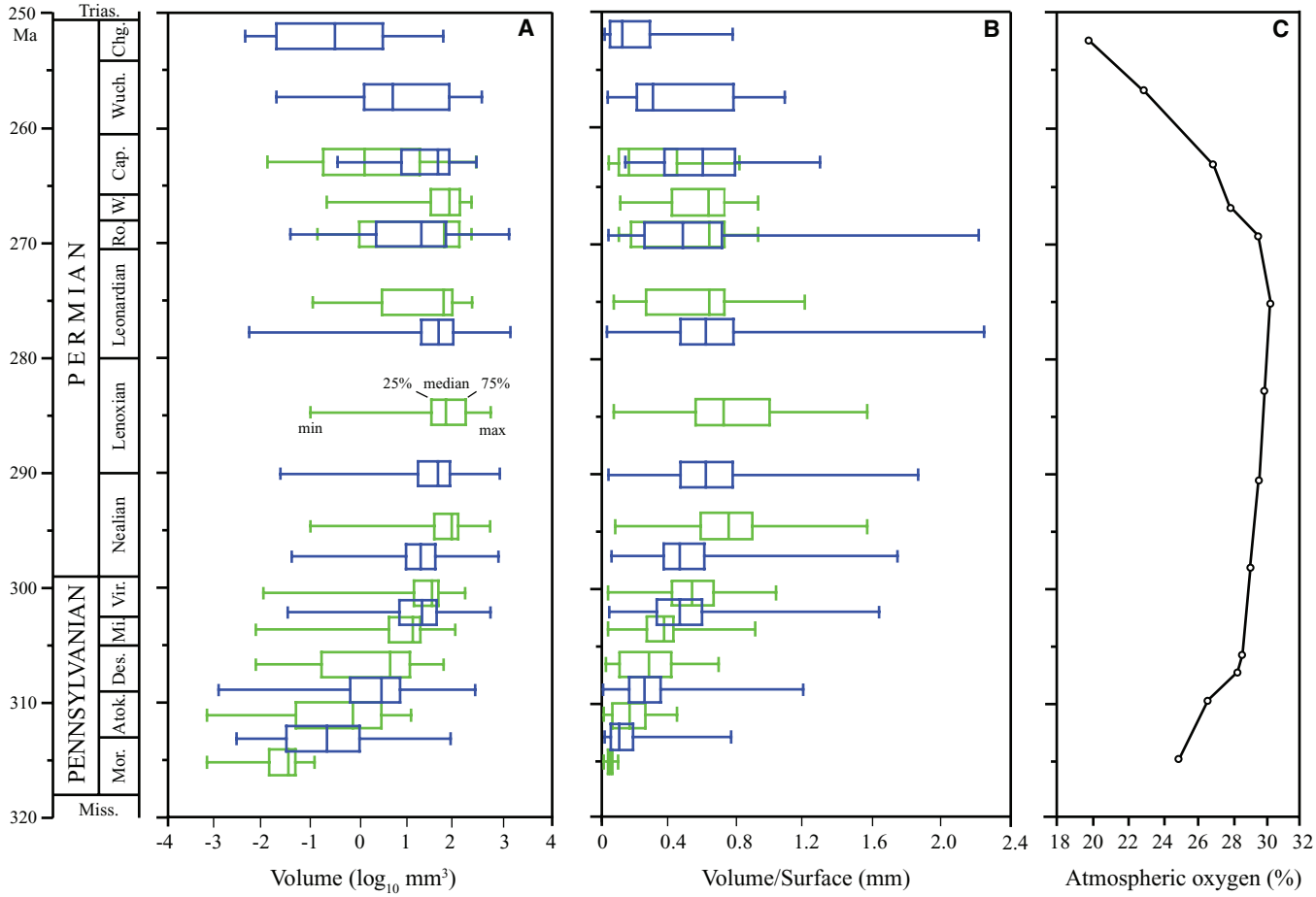

Figure 2. **Pennsylvanian through Permian histories of (A) fusulinoidean volume, (B) volume/surface area ratio, and (C) atmospheric oxygen concentrations estimated from geochemical modeling (Berner 2006). Abbreviations as follows: Mor., Morrowan; Atok., Atokan; Des., Desmoinesian; Mi., Missourian; Vir., Virgilian; Ro., Roadian; W., Wordian; Cap., Capitanian; Wuch., Wuchiapingian; Chg., Changhsingian. Green box plots—North American fusulinoidean data; blue box plots—global fusulinoidean data.**

(4) covaration with atmospheric pO_2. Random walk is the expected mode of size evolution in the absence of selective pressure (McShea 1994). Consistent directional evolution may be expected if larger (or smaller) size is consistently favored, potentially due to intraspecific competitive advantages (Kingsolver and Pfennig 2004). Stasis is expected if size evolution is strongly constrained by invariant selective pressures that cause lower fitness at both larger and smaller sizes. Covariation with atmospheric pO_2 is expected if oxygen availability is an important contributing factor to the relationship between organism size and fitness. There is substantial support in the experimental and comparative biological literature for an influence of oxygen availability on the relationship between size and fitness (reviewed in Payne et al. 2011). Model comparison was run in R (version 2.13.1; R Development Core Team 2011) using the "paleoTS" package (version 0.4–1) (Hunt 2011). Importantly, the analysis is based upon interval-to-interval changes in size (i.e., first differences) rather than raw values, reducing the influence of autocorrelation typical in time series data.

Because the influence of oxygen availability on fitness should increase with size (Fig. 1), we used quantile regression to explicitly assess the correlation between oxygen availability and the upper quantiles of size in our datasets. Quantile regression analyses were conducted using the "quantreg" package (version 4.67) (Koenker 2011). Quantile regression is analogous to ordinary least squares linear regression in assuming a linear relationship between an outcome (in this case, measures of size and shape) and a predictor variable (in this case, oxygen availability). However, it can be used to estimate the relationship between the predictor and any quantile in the outcome.

Results

FUSULINOIDEANS

Both the North American and global datasets indicate that fusulinoidian size increased through the Pennsylvanian (Late Carboniferous), stabilized during the Early and Middle Permian, and declined during the Late Permian (Fig. 2). The size trend broadly

Table 1. Support for models of test size (volume) evolution in fusulinoideans, showing strong support for pO_2 as the main predictor of size.

Model	AICc[1]	Weight
North America		
Directional trend	25.49	0.03
Random walk	23.12	0.09
Stasis	26.62	0.02
pO_2	18.67	0.86
Global		
Directional trend	28.14	0.001
Random walk	25.36	0.004
Stasis	34.55	0.000
pO_2	14.42	0.995

[1] AICc is the small-sample corrected version of Akaike's information criterion, a likelihood-based measure of model fit. AICc weights transform AICc values into proportional support among examined models, which is constrained to sum to 1.

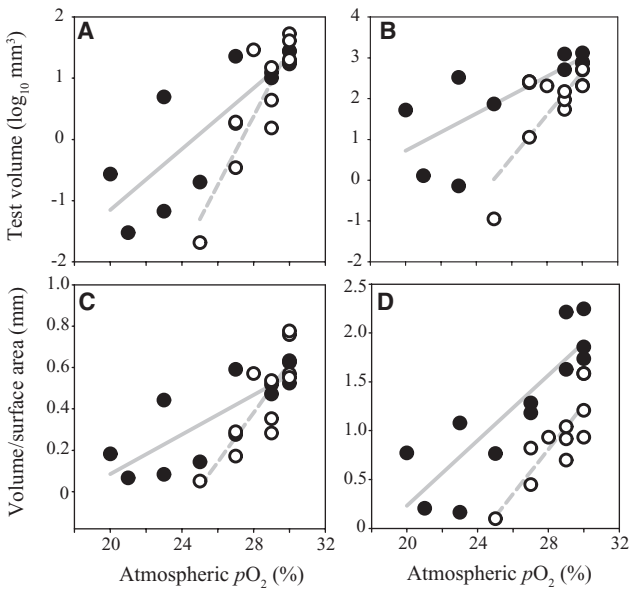

Figure 3. Foraminiferan size and shape parameters correlate with pO_2. (A) mean test volume; (B) maximum test volume; (C) mean volume to surface area ratio; (D) maximum volume to surface area ratio. Filled circles—global dataset; open circles—North American dataset. Regression statistics reported in Table 2.

parallels contemporaneous variations in modeled atmospheric pO_2 (Fig. 2). The similarity of size trends across datasets with differing geographic coverage and degree of taxonomic standardization suggests that the patterns reflect genuine evolutionary trends. Moreover, because size observations in the global dataset are independent from stage to stage (i.e., no size observation is included in more than one geochronologic age), we infer that the distribution of fusulinoidean sizes changed gradually over the same time scale as pO_2 (millions of years).

Evolutionary trends in mean fusulinoidean test (i.e., shell) size across species are better predicted by variation in atmospheric pO_2 than by alternative models based on random walks, consistent directional trends, or stasis (Table 1). The pO_2 model receives 86% of the statistical support for the North American dataset and 99% of the support for the global dataset. In a simple linear model, changes in pO_2 account for more than half of the variance in mean and maximum test volume among species in both datasets (Fig. 3A,B; Table 2). Together, these observations indicate that fusuloinoidean gigantism was more likely a response to environmental change than the result of random drift from a small starting size or inherent ecological advantages associated with larger size.

The relationship between fusulinoidean size and shape is consistent with the scaling analysis presented above. If oxygen transport becomes an increasingly important constraint at larger size, one would expect to find larger species deviating more from spherical geometries to increase relative surface area and maintain relatively short transport distances between the cell surface and interior. Indeed, larger fusulinoideans tend to be less spherical than smaller species, exhibiting larger ratios of maximum to minimum radius at larger size—especially at test volumes greater than 1 mm^3 (Fig. 4). Strictly speaking, oxygen availability limits shape rather than size (i.e., volume); in principle, a foraminiferan cell could have an arbitrarily large volume under the condition that it was a sufficiently thin sheet or cylinder. The fact that few foraminiferan species have ratios of longest to shortest axes greater than three and almost none have ratios greater than 10 explains the observation that oxygen availability correlates not only with the ratio of V/SA but also with volume itself.

V/SA ratios from our North American and global datasets are consistent with expectations based on our scaling analysis. Mean values of V/SA are positively correlated with pO_2 (Fig. 3C) and maximum values are between 1 and 2.25 mm (Fig. 3D), consistent with calculated oxygen transport constraints on fitness. Quantile regression further shows that the 95th percentile of V/SA is significantly associated with pO_2 in both datasets, although the slope of this relationship is subtantially steeper in the North American dataset than the global dataset (Table 3). This difference results largely from the absence of Late Permian data in the North American dataset. Late Permian fusulinoideans are larger than their Carboniferous relatives that lived under similar (or even somewhat higher) oxygen levels (Fig. 1). It is unclear whether the differences in size between Carboniferous and Late Permian fusulinoideans reflects differences in metabolic rate, other selective pressures on cell size, or inaccuracies in reconstructions of pO_2. Despite these complexities, overall the findings described above suggest the

Table 2. Results from linear regression analysis of test size statistics versus atmospheric pO_2.

Mean test volume	Slope	Standard error	*P*-value	Adjusted R^2
North America	0.56	0.102	0.0004	0.75
Global	0.25	0.051	0.0007	0.67
Mean Volume/Surface area ratio				
North America	0.12	0.026	0.0014	0.66
Global	0.048	0.011	0.0014	0.63
Maximum test volume				
North America	0.53	0.123	0.0021	0.63
Global	0.23	0.061	0.0039	0.54
Maximum Volume/Surface area ratio				
North America	0.23	0.047	0.0009	0.69
Global	0.17	0.030	0.0002	0.73

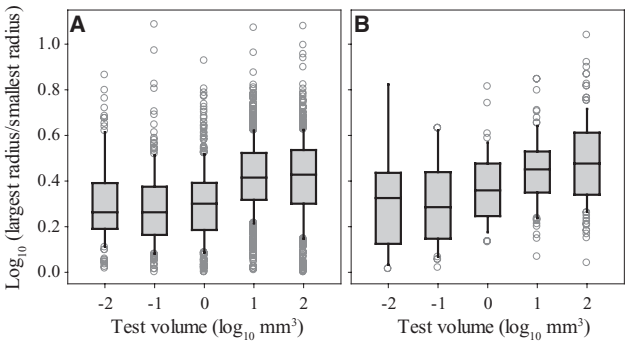

Figure 4. Test size is correlated with aspect ratio (maximum:minimum radius) for the global (A) and North American data (B). Cell shapes become less spherical as overall size becomes larger, consistent with transport-limited physiological models. Boxes indicate 25th, 50th, and 75th percentiles. Whiskers denote the 10th and 90th percentiles. Circles indicate outlying data points. In a simple linear regression analysis, the correlation between aspect ratio and pO_2 is positive and significant for the global dataset (slope = 0.016, $P < 2.2 \times 10^{-16}$) and positive but nonsignificant for the North American dataset (slope = 0.0085, $P = 0.28$).

correlation between fusulinoidean size and pO_2 reflects a direct causal connection rather than an indirect effect or forcing by a shared control.

COMPARISON TO LIVING SPECIES

To further assess the influence of oxygen availability on foraminiferan size, we analyzed data from extant species inhabiting a broad range of dissolved oxygen concentrations on the Sahul Shelf and in the Santa Barbara Basin. This analysis avoids the potential problems from basing our analysis solely on ancient oxygen concentrations estimated from geochemical models, but adds complexity due to differences in the taxa involved and the controls on oxygen availability.

Figure 5 illustrates the size and shape data for the modern species alongside that for the fusulinoidean fossils. The range of test volumes for the Sahul Shelf biota overlaps that of fusulinoideans at similar oxygen concentrations (Fig. 5A). The maximum V/SA ratios of the Sahul Shelf foraminifers follow the same trend with oxygen availability as the fusulinoidean fossils (Fig. 5B). Across the modern data, quantile regression shows a signficant relationship between oxygen availability and the 95th percentile of V/SA (Table 3). However, this relationship results primarily from differences in V/SA and oxygen concentration between the two modern datasets; evidence for a relationship is much weaker within each dataset (Table 3). Variation in dissolved oxygen availability with depth in the modern ocean is an imperfect proxy for long-term variation in atmospheric pO_2 because the depth gradient is correlated to changes in temperature, carbonate saturation level, and nutrient availability in ways that may not be analogous to the fossil datasets. Moreover, the absence of size data for intermediate values of pO_2 prohibits any assessment of potential nonlinear relationships between size or shape and oxygen availability. Consequently, the possibility that the correlation between V/SA and oxygen availability in the modern reflects other controls cannot be ruled out.

Allometric scaling of specific metabolic rate versus cell volume could, in principle, further complicate the relationship of fitness to oxygen availability and cell size. If, for example, specific metabolic rate scales as some exponent b with respect to cell volume, then the fitness contours should be linear in a graph of V^b/SA, rather than V/SA. A recent study of metabolic rate in foraminifera suggests that b may be slightly less than 1 (0.88) in foraminifera (Geslin et al. 2011), although other analyses indicate b may be closer to unity for many other protists (Johnson et al. 2009; DeLong et al. 2010). The fact that protistan metabolic rates scale with cell volume following an exponent close to 1 indicates that our conclusions regarding the general relationship between V/SA and oxygen availability are not senstive to the precise value of b.

Table 3. Results from quantile regression analysis of 95th percentile of volume to surface area ratio (V/SA) versus oxygen concentration.

Dataset	Intercept	Standard Error	Slope	Standard Error	*P*-value
All data	−0.03	0.0002	0.032	<0.0001	<0.0001
Fossil	−1.35	0.19	0.079	0.0067	<0.0001
Modern	−0.03	0.12	0.038	0.0102	0.0002
Global Fusulinoidean	−1.18	0.19	0.073	0.0066	<0.0001
North America fusulinoidean	−5.29	1.01	0.22	0.036	<0.0001
Sahul Shelf	0.00	0.0008	0.002	0.0008	0.017
Santa Barbara Basin	0.25	0.07	0.0006	0.0037	0.87

Discussion

Beyond the strong correlation between fusulinoidean size and atmospheric pO_2, our data also indicate that pO_2 was far from the only influence on fusulinoidean size evolution. The enormous range of fusulinoidean sizes within each time interval highlights the continued importance of biotic interactions and local environmental conditions in controlling size evolution within individual lineages. The correlation of maximum and mean fusulinoidean size with atmospheric pO_2 despite the enormous range of sizes exhibited within each time interval shows that these local effects were not strong enough to overwhelm the influence of global environmental change on the relationship between size and fitness.

Fusulinoideans are widely hypothesized to have harbored photosymbiotic algae (Ross 1972; Lee and Hallock 1987; Groves and Wang 2009), potentially complicating the influence of extracellular oxygen concentration to cell size and fitness. For example, oxygen production by macroalgae can significantly influence development in attached animal egg masses (Woods and Podolsky 2007; Fernandes and Podolsky 2011), at least partially decoupling them from the broader external environment. However, several lines of evidence beyond the observed correlation between pO_2 and fusulinoidean size indicate that photosymbionts do not eliminate the influence of extracellular oxygen availability on cell size and fitness. First, as calculated above, oxygen is mixed througout the cell on a time scale of minutes by cytoplasmic streaming; consequently, foraminifera cannot maintain oxygen concentrations above extracellular values througout the dark hours. In contrast, oxygen transport times in animal egg masses are substantially longer because the eggs are housed in gelatinous masses and thus depend primarily on diffusion for oxygen supply. Second, extant symbiont-bearing foraminifera quickly become oxygen sinks in the absence of light (Köhler-Rink and Kühl 2000). Third, even some symbiont-bearing foraminifers are net consumers of oxygen (Walker et al. 2011). Finally, the earliest fusulinoideans were not unusually large relative to their closest relatives. The earliest fusulinoideans (Visean) were similar in size to nonfusulinoidean members of Order Fusulinida from the Visean and the previous stage (Tournaisian), as well as all Visean foraminifera from the Ellis and Messina catalog (Fig. 6). These observations suggest that there is no simple relationship between photosymbiosis and gigantism in fusulinoideans. Early fusulinoideans may have harbored photosymbionts but maintained small sizes or, alternatively, acquistion of photosymbionts may have occurred later in the evolutionary history of this group. The dramatic size increase occurred later, during the Atokan (=late Bashkirian/early Moscovian) age. This corresponds precisely with the advent of a fusiform shape, suggesting either a link between photosymbiosis and cell size or, alternatively, the constraints imposed by larger size on V/SA ratios.

The correlation between foraminiferan size and oxygen availability observed in this study is consistent with previous studies on both fossil and living material. In the modern oceans, low oxygen settings are typically associated with thinner-shelled, smaller, and less spherical species and individuals (Kaiho 1994; Gooday et al. 2000, 2009). The sizes of the Holocene Santa Barbara Basin specimens from our study are comparable to those from the oxygen minimum zone of the Arabian Sea (cf. Gooday et al. 2000), confirming that our findings are not contingent upon factors particular to the Santa Barbara Basin. Kaiho (1994) used the strong correspondence between seawater oxygen concentrations and benthic foraminiferan community composition and morphology in the modern oceans to develop a dissolved-oxygen index that could be applied to paleoceanographic problems using fossil material. Using this index, Kaiho (1998) found that the maximum sizes of deep-sea, trochospiral, benthic foraminifers covaried with benthic seawater temperatures over the past 120 million years, and interpreted this relationship to indicated that temperature-driven controls on oxygen availability influenced the size evolution of deep-sea benthic foraminifera.

The influences of hyperoxia on fusulinoidean evolution may have extended beyond enabling large size. Fusulinoideans are remarkable as much for their extraordinary abundance and diversity as for their large size. We hypothesize that hyperoxia also affected these aspects of fusulinoidean evolution. Enhanced oxygenation of Carboniferous and Permian seawater would have affected

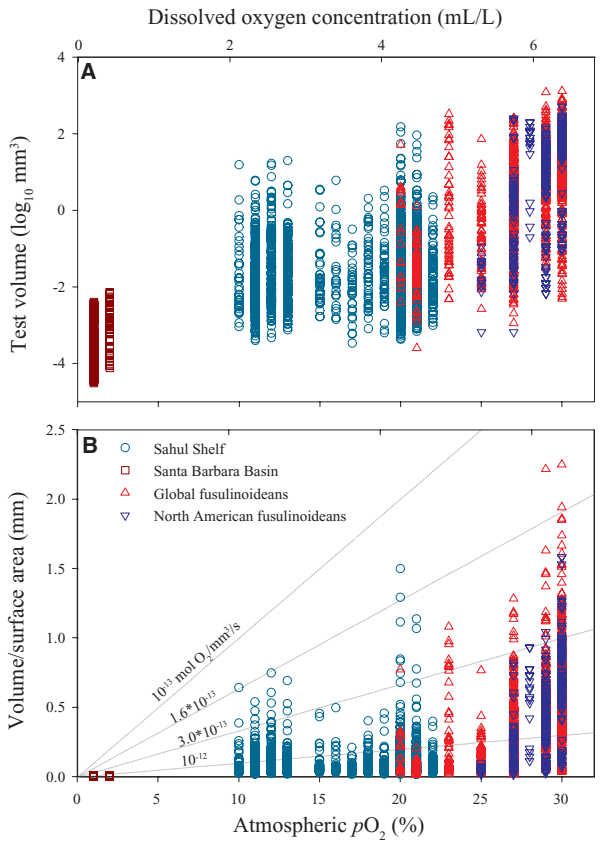

Figure 5. Extant foraminifera along an oxygen gradient follow a similar trend as in the fossil record. Test volume (A) and volume to surface area (V/SA) ratio (B) versus oxygen availability (expressed for simplicity as pO_2 in equilibrium with seawater at 25°C) for living and fossil foraminifers. Extant species were sampled along an oxygen gradient on the Sahul Shelf and from oxygen minimum zone sediments in the Santa Barbara Basin. As noted in the text, the maximum V/SA is directly proportional to the cytoplasmic streaming rate and external oxygen concentration and inversely proportional to the metabolic rate. The dotted lines indicate contours of predicted maximum V/SA as a function of metabolic rate, assuming a cytoplasmic streaming rate of $5{\cdot}10^{-3}$ mm/sec. Given the fact that species and individuals will differ in rates of cytoplasmic streaming and aerobic metabolism, these lines should not be viewed as upper bounds on size; rather, they should be interpreted as contours of approximately equivalent selective pressure from the physiological contraints on oxygen supply and demand. The size typical of any given species will depend upon the oxygen-induced selective pressures as well as any other size-dependent physiological and ecological factors. Oxygen concentrations in seawater for fusulinoideans assume atmospheric equilibrium with seawater at 25°C.

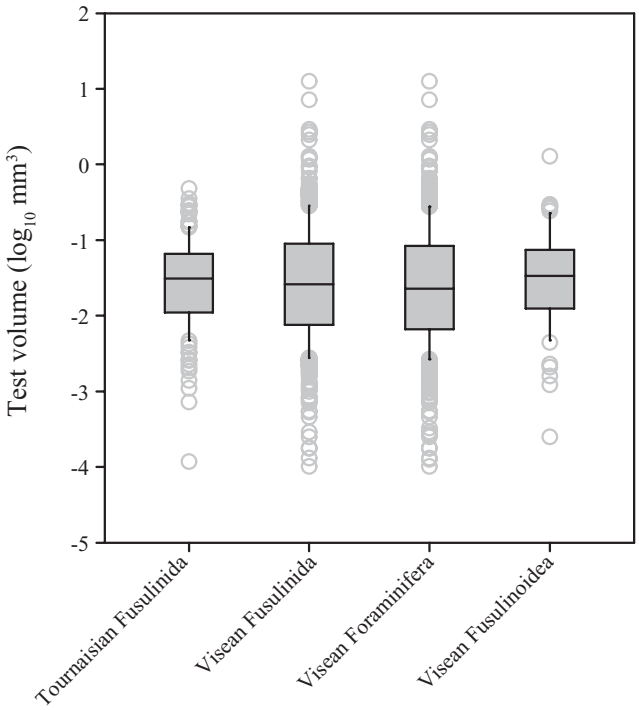

Figure 6. Size distribution of the earliest fusulinoideans (Visean) from the Ellis and Messina catalog compared to that of all members of Order Fusulinida for the Visean and the previous stage (Tournaisian), as well as all Visean foraminiferan species, showing that the earliest members of superfamily Fusulinoidea were not unusually large (or small) relative to their closest relatives. Boxes indicate 25th, 50th, and 75th percentiles. Whiskers denote the 10th and 90th percentiles. Circles indicate outlying data points.

nutrient availability because the efficiency of phosphate burial is associated with seawater redox state. Phosphorus is efficiently trapped in sediments as a ferric oxide under oxygenated conditions whereas it is more efficiently returned to the water column under anoxic conditions (Van Cappellen and Ingall 1996). If most or all fusulinoideans did harbor photosymbionts (Ross 1972; Lee and Hallock 1987; Groves and Wang 2009) and symbiotic associations are particularly favored in low-nutrient environments (Hallock 1981) where phosphate is often limiting, then expansion of oligotrophic environments driven by atmospheric hyperoxia may have provided an environment both permissive of gigantism and favorable to fusulinoideans.

The correlation between fusulinoidean size and atmospheric pO_2 during late Paleozoic time is consistent with long-standing speculation that hyperoxia enabled gigantism, but the extent to which fusulinoidean evolution is representative of other coexisting taxa remains unclear for several reasons. First, although very large insects, marine invertebrates, and large tetrapods all lived during Carboniferous and Permian time, comparably detailed records of size change do not exist for any of these other groups. Consequently, the extent to which sizes increased (and decreased) in concert remains unknown. Giant insects, such as the dragonfly *Meganeura*, occur in Pennsylvanian and Permian rocks (Graham et al. 1995), broadly coeval with fusulinoidean gigantism, whereas the famously large brachiopod *Gigantoproductus* occurs in Visean rocks (~335 Mya) (Williams et al. 2000–2007),

predating size increase in fusulinoideans and the major rise in pO_2. Many other marine animal groups exhibit size maxima long prior to the Permo–Carboniferous; for example, the largest Paleozoic cephalopod, gastropod, and trilobite all occur in Ordovician rocks (Teichert and Kummel 1960; Rohr et al. 1992; Rudkin et al. 2003). Second, it is challenging to calculate oxygen-imposed size maxima for animals due to their more complex respiratory anatomy (e.g., Kaiser et al. 2007). Thus, it is difficult to distinguish the effects on size attributable to biotic interactions from those attributable to environmental conditions in the absence of comprehensive size data. Existing evidence suggests biotic interactions may impose important constraints on maximum size in some taxa. For example, the differences in size between the largest Permo–Carboniferous and living dragonflies are much too large to be accounted for by change in atmospheric pO_2 alone, suggesting competition with flying vertebrates has imposed limits on maximum dragonfly size far below the physiologically allowable maximum for the past 250 million years (Okajima 2008).

Although it remains unclear whether late Paleozoic gigantism represents a unified response of the biosphere to atmospheric hyperoxia, the correlation of fusulinoidean sizes with reconstructed atmospheric oxygen levels, calculations indicating that fusulinoidean fitness could be affected by morphological constraints on oxygen uptake, and comparative analysis of living foraminifers showing similar morphological responses to oxygen availability, all indicate that atmospheric hyperoxia enabled fusulinoidean gigantism.

ACKNOWLEDGMENTS

We thank D. Perrett, X. Ouyang, N. DeVille, F. Caval-Holme, J. Binn, M. Erviti, J. Campbell, A. Garcia, S. Lo, S. Smith, N. O'Keefe, K. Cheung, G. Haq, D. Foster, D. Gomez, D. Guo, A. Jin, K. Ingram, C. Khong, E. Barnosky, and S. Sanghvi for assistance in data collection and J. Kennett for access to samples from core MD02-2503. This work was supported by the donors to the Petroleum Research Fund of the American Chemical Society (50639-UR8 to J. R. Groves), grants from the Stanford University Vice Provost for Undergraduate Research (J. L. Payne and J. M. Skotheim), Stanford University Bio-X Interdisciplinary Initiative Program (J. L. Payne and J. M. Skotheim), NSF (CAREER Award #1054025 to J. M. Skotheim), and the Burroughs Wellcome Fund (J. M. Skotheim).

LITERATURE CITED

Alroy, J. 1998. Cope's rule and the dynamics of body mass evolution in North American fossil mammals. Science 280:731–734.

Berner, R. A. 1987. Models for carbon and sulfur cycles and atmospheric oxygen; application to Paleozoic geologic history. Am. J. Sci. 287:177–196.

———. 2006. GEOCARBSULF: a combined model for Phanerozoic atmospheric O_2 and CO_2. Geochim. Cosmochim. Acta 70:5653–5664.

Berner, R. A., and D. E. Canfield. 1989. A new model for atmospheric oxygen over Phanerozoic time. Am. J. Sci. 289:333–361.

Berner, R. A., J. M. VandenBrooks, and P. D. Ward. 2007. Oxygen and evolution. Science 316:557–558.

Clauset, A., and D. H. Erwin. 2008. The evolution and distribution of species body size. Science 321:399–401.

Cope, E. D. 1871. The method of creation of organic forms. Proc. Am. Philos. Soc. 12:229–263.

Coulbourn, W. T., and J. M. Resig. 1975. On the use of benthic foraminifera as sediment tracers in a Hawaiian bay. Pac. Sci. 29:99–115.

DeLong, J. P., J. G. Okie, M. E. Moses, R. M. Sibly, and J. H. Brown. 2010. Shifts in metabolic scaling, production, and efficiency across major evolutionary transitions of life. Proc. Natl. Acad. Sci. USA 107:12941–12945.

Douglass, R. C. 1977. The development of fusulinid biostratigraphy. Pp. 463–482 *in* E. G. Kauffman, and J. E. Hazel, eds. Concepts and methods of biostratigraphy. Dowden Hutchinson and Ross, Stroudsburg, PA.

Dudley, R. 1998. Atmospheric oxygen, giant Paleozoic insects and the evolution of aerial locomotor performance. J. Exp. Biol. 201:1043–1050.

Dunbar, C. O. 1963. Trends of evolution in American fusulines. Pp. 25–44 *in* G. H. R. von Koenigswald, J. D. Emeis, W. L. Buning, and C. W. Wagner, eds. Evolutionary trends in foraminifera. Elsevier, Amsterdam.

Ellis, B. F., and A. R. Messina. 1940. Catalogue of foraminifera. The American Museum of Natural History, New York.

Fernandes, D. A. O., and R. D. Podolsky. 2011. Developmental consequences of association with a photosynthetic substrate for encapsulated embryos of an intertidal gastropod. J. Exp. Mar. Biol. Ecol. 407:370–376.

Fieux, M., C. Andrie, P. Delecluse, A. G. Ilahude, A. Kartavtseff, F. Mantisi, R. Molcard, and J. C. Swallow. 1994. Measurements within the Pacific-Indian oceans throughflow region. Deep-Sea Res., Part I 41:1091–1130.

Geslin, E., N. Risgaard-Petersen, F. Lombard, E. Metzger, D. Langlet, and F. Jorisson. 2011. Oxygen respiration rates of benthic foraminifera as measured with oxygen microsensors. J. Exp. Mar. Biol. Ecol. 396:108–114.

Gooday, A. J., J. M. Bernhard, L. A. Levin, and S. B. Suhr. 2000. Foraminifera in the Arabian Sea oxygen minimum zone and other oxygen-deficient settings: taxonomic composition, diversity, and relation to metazoan faunas. Deep-Sea Res., Part I 47:25–54.

Gooday, A. J., L. A. Levin, A. Aranda da Silva, B. J. Bett, G. L. Cowie, D. Dissard, J. D. Gage, D. J. Hughes, R. Jeffreys, P. A. Lamont, et al. 2009. Faunal responses to oxygen gradients on the Pakistan margin: a comparison of foraminiferans, macrofauna and megafauna. Deep-Sea Res., Part II 56:488–502.

Gould, S. J. 1988. Trends as changes in variance – a new slant on progress and directionality in evolution. J. Paleontol. 62:319–329.

Gradstein, F. M., and J. G. Ogg. 1996. A Phanerozoic time scale. Episodes 19:3–5.

Graham, J. B., N. M. Aguilar, R. Dudley, and C. Gans. 1995. Implications of the late Paleozoic oxygen pulse for physiology and evolution. Nature 375:117–120.

Groves, J. R., and Y. Wang. 2009. Foraminiferal diversification during the late Paleozoic ice age. Paleobiology 35:367–392.

Hallock, P. 1981. Algal symbiosis: a mathematical analysis. Mar. Biol. 62:249–255.

Hunt, G. 2006. Fitting and comparing models of phyletic evolution: random walks and beyond. Paleobiology 32:578–601.

Hunt, G., S. A. Wicaksono, J. E. Brown, and K. G. Macleod. 2010. Climate-driven body-size trends in the ostracod fauna of the deep Indian ocean. Palaeontology 53:1255–1268.

Hunt, G., 2011. paleoTS: analyze paleontological time-series. R package version 0.4–1. Available at http://CRAN.R-project.org/package=paleoTS. (accessed February 2, 2012).

Ivanochko, T. S., and T. F. Pedersen. 2004. Determining the influences of late quaternary ventilation and productivity variations on Santa Barbara basin sedimentary oxygenation: a multi-proxy approach. Quat. Sci. Rev. 23:467–480.

Johnson, M. D., J. Volker, H. V. Moeller, E. Laws, K. J. Breslauer, and P. G. Falkowski. 2009. Universal constant for heat production in protists. Proc Natl Acad Sci USA 106:6696–6699.

Kaiho, K. 1994. Benthic foraminiferal dissolved-oxygen index and dissolved-oxygen levels in the modern ocean. Geology 22:719–722.

———. 1998. Global climatic forcing of deep-sea benthic foraminiferal test size during the past 120 m.y. Geology 26:491–494.

Kaiser, A., C. J. Klok, J. J. Socha, W.-K. Lee, M. C. Quinlan, and J. F. Harrison. 2007. Increase in tracheal investment with beetle size supports hypothesis of oxygen limitation on insect gigantism. Proc. Natl. Acad. Sci. USA. 104:13198–13203.

Kingsolver, J. G., and D. W. Pfennig. 2004. Individual-level selection as a cause of Cope's rule of phyletic size increase. Evolution 58:1608–1612.

Koenker, R. 2011. quantreg: quantile regression. R package version 4.76. Available at http://CRAN.R-project.org/package=quantreg.

Köhler-Rink, S., and M. Kühl. 2000. Microsensor studies of photosynthesis and respiration in larger symbiontic foraminifera, I. The physicochemical microenvironment of *Marginopora vertebralis*, *Amphistegina lobifera* and *Amphisorus hemprichii*. Mar. Biol. 137:473–486.

Lee, J. J., and P. Hallock. 1987. Algal symbiosis as the driving force in the evolution of larger foraminifera. Ann. NY Acad. Sci. 503:330–347.

Loeblich, A. R., and H. Tappan. 1994. Foraminifera of the Sahul Shelf and Timor Sea. Spec. Pub.—Cushman Found. Foraminiferal Res. 31:1–661.

McShea, D. W. 1994. Mechanisms of large-scale evolutionary trends. Evolution 48:1747–1763.

Newell, N. D. 1949. Phyletic size increase, an important trend illustrated by fossil invertebrates. Evolution 3:103–124.

Ogg, J. G., G. Ogg, and F. M. Gradstein. 2008. The concise geologic time scale. Cambridge Univ. Press, Cambridge, UK.

Okajima, R. 2008. The controlling factors limiting maximum body size of insects. Lethaia 41:423–430.

Payne, J. L., A. G. Boyer, J. H. Brown, S. Finnegan, M. Kowalewski, R. A. Krause, S. K. Lyons, C. R. McClain, D. W. McShea, P. M. Novack-Gottshall, et al. 2009. Two-phase increase in the maximum size of life over 3.5 billion years reflects biological innovation and environmental opportunity. Proc. Natl. Acad. Sci. USA 106:24–27.

Payne, J. L., C. R. McClain, A. G. Boyer, J. H. Brown, S. Finnegan, M. Kowalewski, R. A. Krause, S. K. Lyons, D. W. McShea, P. M. Novack-Gottshall, et al. 2011. The evolutionary consequences of oxygenic photosynthesis: a body size perspective. Photosynth. Res. 107:37–57.

Poelaert, D., J. Schniewind, and F. Janssens. 2011. Surface area and curvature of the general ellipsoid. arXiv.org/abs/1104,5145.

R Development Core Team. 2011. R: a language and environment for statistical computing. R Foundation for Statistical Computing, Vienna, Austria. Available at ISBN 3–900051-07–0, URL http://www.R-project.org/. (accessed February 2, 2012).

Rohr, D. M., R. B. Blodgett, and W. M. Furnish 1992. *Maclurina manitobensis* (Whiteaves) (Ordovician Gastropoda); the largest known Paleozoic gastropod. J. Paleontol. 66:880–884.

Ross, C. A. 1972. Paleobiological analysis of fusulinacean (Foraminiferida) shell morphology. J. Paleontol. 46:719–728.

Royer, D. L., R. A. Berner, I. P. Montañez, N. J. Tabor, and D. J. Beerling. 2004. CO_2 as a primary driver of Phanerozoic climate. GSA Today 14:4–10.

Rudkin, D. M., G. A. Young, R. J. Elias, and E. P. Dobrzanski. 2003. The world's biggest trilobite—*Isotelus rex* new species from the upper Ordovician of northern Manitoba, Canada. J. Paleontol. 77:99–112.

Rutten, M. G. 1966. Geologic data on atmospheric history. Palaeogeogr. Palaeoclimatol. Palaeoecol. 2:47–57.

Schidlowski, M., and C. E. Junge. 1981. Coupling among the terrestrial sulfur, carbon and oxygen cycles: numerical modeling based on revised Phanerozoic carbon isotope record. Geochim. Cosmochim. Acta 45:589–594.

Schidlowski, M., C. E. Junge, and H. Pietrek. 1977. Sulfur isotope variations in marine sulfate evaporites and the Phanerozoic oxygen budget. J. Geophys. Res. 82:2557–2565.

Sholkovitz, E. R., and J. M. Gieskes. 1971. A physical-chemical study of the flushing of the Santa Barbara Basin. Limnol. Oceanogr. 16:479–489.

Simpson, G. G. 1944. Tempo and mode in evolution. Columbia Univ. Press, New York.

Stanley, S. M. 1973. An explanation for Cope's rule. Evolution 27:1–26.

Stevens, C. H. 1995. A giant Permian fusulinid from east-central Alaska with comparisons of all giant fusulinids in western North America. J. Paleontol. 69:805–812.

Strathmann, R. R., and M. F. Strathmann. 1995. Oxygen supply and limits on aggregation of embryos. J. Mar. Biol. Assoc. UK 75:413–428.

Subczynski, W. K., J. S. Hyde, and A. Kusumi. 1989. Oxygen permeability of phosphatidylcholine–cholesterol membranes. Proc. Natl. Acad. Sci. USA 86:4474–4478.

———. 1991. Effect of alkyl chain unsaturation and cholesterol intercalation on oxygen transport in membranes: a pulse ESR spin labeling study. Biochemistry 30:8578–8590.

Subczynski, W. K., and H. M. Swartz. 2005. EPR oximetry in biological and model samples. Biol. Magn. Reson. 23:229–282.

Teichert, C., and B. Kummel. 1960. Size of endoceroid cephalolopods. Breviora Mus. Comp. Zool. 128:1–7.

Travis, J. L., and S. S. Bowser. 1991. The motility of foraminifera. Pp. 91–155 *in* J. J. Lee, and O. R. Anderson, eds. Biology of foraminifera. Academic Press, San Diego.

Van Cappellen, P., and E. D. Ingall. 1996. Redox stabilization of the atmosphere and oceans by phosphorus-limited marine productivity. Science 271:493–496.

Walker, R. A., P. Hallock, J. J. Torres, and G. A. Vargo. 2011. Photosynthesis and respiration in five species of benthic foraminifera that host algal endosymbionts. J. Foram. Res. 41:314–325.

White, D. C. S. 1974. Biological physics. Chapman and Hall, London.

Williams, A., C. H. C. Brunton, and S. J. Carlson, eds. 2000–2007. Treatise on invertebrate paleontology. Part H, Brachiopoda. Geological Society of America and Paleontological Institute, Boulder, CO.

Woods, H. A., and R. D. Podolsky. 2007. Photosynthesis drives oxygen levels in macrophyte-associated gastropod egg masses. Biol. Bull. 213:88–94.

Associate Editor: M. Hart